ELSEVIER

Journal of Electron Spectroscopy and Related Phenomena 98–99 (1999) 335–343

JOURNAL OF ELECTRON SPECTROSCOPY and Related Phenomena

Conductance through atomic contacts created by scanning tunneling microscopy

Ç. Kiliç[a], H. Mehrez[a], S. Ciraci[a], Inder P. Batra[b,*☆]

[a]*Department of Physics, Bilkent University, Bilkent 06533, Ankara, Turkey*
[b]*IBM Almaden Research Center, San Jose, California 95120-6099, USA*

Received 11 October 1997; accepted 31 January 1998

Abstract

We investigate conductance through contacts created by pressing a hard tip, as used in scanning tunneling microscopy, against substrates. Two different substrates are considered, one a normal metal (Cu) and another a semi-metal (graphite). Our study involves the molecular dynamics simulations for the atomic structure during the growth of the contact, and selfconsistent field electronic structure calculations of deformed bodies. We develop a theory predicting the conductance variations as the tip approaches the surface. We offer an explanation for a quasiperiodic variation of conductance of the contact on the graphite surface, a behavior which is dramatically different from contacts on normal metals. © 1999 Elsevier Science B.V. All rights reserved.

Keywords: Atomic contacts; Conductance; Molecular dynamics simulations

1. Introduction

Brundle has been a pioneer in developing and applying spectroscopic techniques, UPS in particular, to a variety of fundamental as well as applied problems. Our collaborative work [1,2]. spanned a period of more than a decade when we (IPB and CR13) both worked at IBM Almaden Research Center in the physical sciences department. We were most interested in investigating the interactions of atoms and molecules with surfaces. More specifically, the objective was to deduce atomic arrangements from the modified electronic properties which the adsorbates (and surfaces) suffered when brought within a few Å of each other. The work we present here to honor Brundle still deals with bringing atoms close to a surface, but has an entirely new focus. We employ scanning tunneling microscopy (STM) to create contacts of atomic widths and study conductance through such "atomic" wires. The electron transport through an atomic size contact is important not only for a better understanding of mesoscopic physics, but also for novel device applications. While the tunneling current in STM can probe the local density of states at E_F and is used also as a spectroscopic tool, the transport through a contact can provide valuable information about both electronic and atomic structures.

The size of the contact width created by a sharp metal tip on metal surfaces is set by a single atom at the apex of the STM tip and has a typical radius, $R_c = 2$–4 Å. The contact size grows as the tip is pushed closer towards the sample. For typical metallic

* Corresponding author. Tel.: + 1-312-413-2798; Fax: + 1-312-996-9016; e-mail: ipbatra@uic.edu

☆ Present address: Department of Physics, University of Illinois at Chicago, Chicago, Illinois 60607-7059, USA.

0368-2048/98/$ - see front matter © 1999 Elsevier Science B.V. All rights reserved.
PII: S0368-2048(98)00297-7

charge densities, the contact diameter, $2R_c$, is in the range of the Fermi wavelength λ_F. In this length scale the level spacing of electron energy eigenstates (transversally confined to the contact) is approximately, 1 eV. The discrete structure of the contact leads to observable variations in mechanical and electronic properties whenever there is any change in its size and atomic arrangement. In particular, the two terminal conductance G of a contact has shown discontinuous (sudden) variations while the tip is pushed continuously [3–11]. Similar behavior has been obtained in a connective neck that was formed by the tip retracting from an indentation [12–17].

As far as the electronic transport is concerned, an atomic size contact or connective neck can be viewed as a constriction with length l smaller than the mean free path of the electron, l_e, and $R_c \sim \lambda_F$, where the motion of electrons is confined in the transversal direction. Whether the two terminal ballistic conductance through such a constriction is quantized, has been controversial [8, 9, 18 ,19]. Most recent studies have revealed various yielding mechanisms and resulting novel atomic structure during the evolution of the contact when the tip moves towards or pulls away from the surface [20–24].

We investigate the electronic conductance through an atomic size point contact created by a sharp STM metal tip with two different metallic surfaces having different electronic properties. The samples we consider are the Cu(001) surface, a typical metal, and the graphite (0001), a layered material. The contacts on metal surfaces have been investigated both experimentally and theoretically [12–17]. Measurements [25] of the conductance of a contact created on the graphite surface showed unexpected results. Instead of rising with the push of the tip, G oscillated between high and low values. This observation has been known in private circles but no publication exists perhaps due to an insufficient understanding of the phenomenon. An objective of the present study is then to explain the variation of *G(s)*. To this end we first outline the theory of the ballistic conduction mechanism in an atomic size constriction by clarifying the concept of quantized conductance. We then examine the growth of the contact in those two different types of sample surfaces by using molecular dynamics (MD) simulations. Based on the atomic structure obtained from the MD simulations and the results of the electronic structure calculations we deduce the variation of conductance, G with the displacement of the tip towards sample.

2. Ballistic conductance in a constriction

To elucidate the concept of quantized conductance we consider a uniform quasi 1D constriction (along z) between two 2D (yz) electron gas reservoirs with the infinite wall confining potential. The motion of an electron in the transversal (y)direction is confined, but it can propagate freely along the z direction. The current transporting states are constructed in terms of the confined and propagating constriction states. The upper limit for the conductance of a current transporting state with the transmission coefficient, $T = 1$ was deduced by Batra [26] from the uncertainty principle. The current transmitted by such a state in the quantum limit is $I = 2e/\Delta t$ for both spins. Then the conductance $G = I/\Delta V = 2e^2/(\Delta t e \Delta V)$. Since $e\Delta V = \Delta E$ and $\Delta t \Delta E \geq h$, the upper limit is

$$G \leq \frac{2e^2}{h} \tag{1}$$

We note that this upper limit from uncertainty principle is reached for eigenstates which are plane wave like.

In the reservoirs, the mean charge density, ρ_e, determines the Fermi energy, E_F and hence λ_F since $E_F = (h^2/2m^*)\lambda_F^{-2}$ The first constriction state that is transversally confined, $\Phi_{i=1}(y)$ becomes occupied (i.e. $\epsilon_{i=\tilde{1}} \leq E_F$) if the width of the constriction with the confining potential, $w \geq \lambda_F/2$. The longitudinal wave propagates along z with the propagation constant $\gamma_i = [(2m^*/\hbar^2)(E_F - \varepsilon_i)]^{1/2}$. Therefore, whenever w increases by $\lambda_F/2$, a new sub-band dips below the Fermi level. With this background one can easily calculate the conductance of the uniform constriction of infinite length. The current under small bias voltage ΔV,

$$I = \sum_{i=1}^{j} 2n_i e v_{\gamma i}[D_i(E_F + e\Delta V) - D_i(E_F)] \tag{2}$$

Here j is the index of the highest occupied sub-band that lies below the Fermi level, i.e. $\epsilon_j \leq E_F$ and $\epsilon_{j+1} > E_F$, and n_i, is the degeneracy of the state i. By

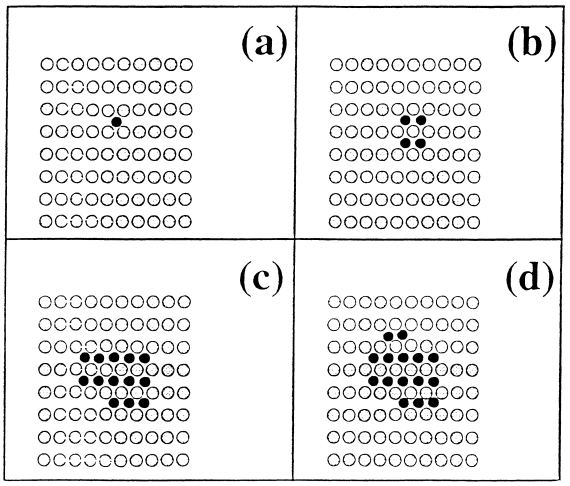

Fig. 1. The top view of the atomic structure of the contact interface created by the Ni(111) tip on the Cu(001) metal substrate. As the tip is pushed towards the substrate, the interface grows discontinuously from (a) to (d). The Ni and Cu atoms are indicated by filled and empty circles, respectively. The positions of atoms are calculated by molecular dynamics simulations performed at 4 K.

assuming $T = 1$, and expressing the group velocity, v_{γ_i}, and the density of states, $D_i(\epsilon)$ in terms of the sub-band energy $\varepsilon = \varepsilon_i + [(\hbar^2\gamma_i^2)/(2m^*)]$ and dividing I by ΔV we obtain

$$G = \sum_{i=1}^{j} \frac{2e^2}{h} n_i \tag{3}$$

Therefore each current carrying state with energy, ε_i, $(E_F < \varepsilon_i < E_F + e\Delta V)$ contributes to G by $2e^2 n_i/h$. For the uniform, infinite wall constriction the degeneracy $n_i = 1$, and hence the increase of w by $\lambda_F/2$ causes G to jump by $2e^2/h$. As a result, the G(w) curve exhibits a staircase structure. This variation for $l < l_e$, is identified with the usual quantization of conductance.

The measurements of the conductance G through a narrow constriction between two reservoirs of 2D electron gas in high mobility GaAs–GaAlAs heterostructure confirmed the above theories [27, 28]. The constriction made by a split gate was significantly narrow ($w = 2500$ Å in the range of Fermi wave length corresponding to a low density in a 2D electron gas system) and also short ($l < l_e$) so that electrons can move ballistically and their transversally confined motion are quantized as explained above. Subsequent theoretical studies [10] noted that the level spacing $\Delta\epsilon \sim \lambda_F^{-2}$, which is rather small for the low electron density in the 2D electron gas system, the sharp step structure is likely to be smeared out at $T \sim 10$ K or at finite bias voltage ΔV. Also, the effects, such as saddle point of the electronic potential, surface roughness, impurity scattering, will cause the sharp step structure of *G(w)* to disappear. The length of the constriction is another important parameter. In order to get sharp step structure l has to be greater than λ_F; *G(w)* is smoothed out in short ($l < \lambda_F$) constrictions. In summary, *G(w)* exhibits sharp step structure if the constriction is uniform, $w \sim \lambda_F$ and $\lambda_F \ll l < l_e$

3. Atomic contacts on metal surfaces

The point contact between a metal tip and surface represents a short but non-uniform constriction with high electron density, ρ_e, and hence very short λ_F (~ 5–8 Å). Even the single atom at the apex of the tip can create contact with a diameter $2R_c \sim \lambda_F$. In such a contact the motion of the electrons is confined in the (*xy*)plane, but free in the *z* direction. Since in the usual metallic charge densities $\lambda_F \sim 5$–8 Å, and the level spacing is large (~ 1 eV), the channels do not mix at room temperature ($T \sim 300$ K). But for $l < \lambda_F$ the atomic structure is highly irregular.

Almost three decades ago Sharvin [29] investigated a very short point contact by using a semi-classical approach and showed that the conductance is independent of any material properties and is solely determined by the geometry (or cross-section A) of the contact and mean electron density of the reservoir, ρ_e. The expression he derived (which is now referred to as the Sharvin's conductance) is given by

$$G_S = \left(\frac{2e^2}{h}\right)\left(\frac{\pi R_c}{\lambda_F}\right)^2 \tag{4}$$

It increases linearly with A. While the Sharvin's expression adequately describes the ballistic conductance of a contact of large A, it violates the uncertainty principle for $A \ll \pi\lambda_F^2$. In the quantum regime, where $A \sim \lambda_F^2$, G_S should vanish for $A < A_c$, some threshold cross-section (A_c) which is determined by the uncertainty principle.

For a circularly symmetric, uniform and long constriction with infinite wall potential the variation

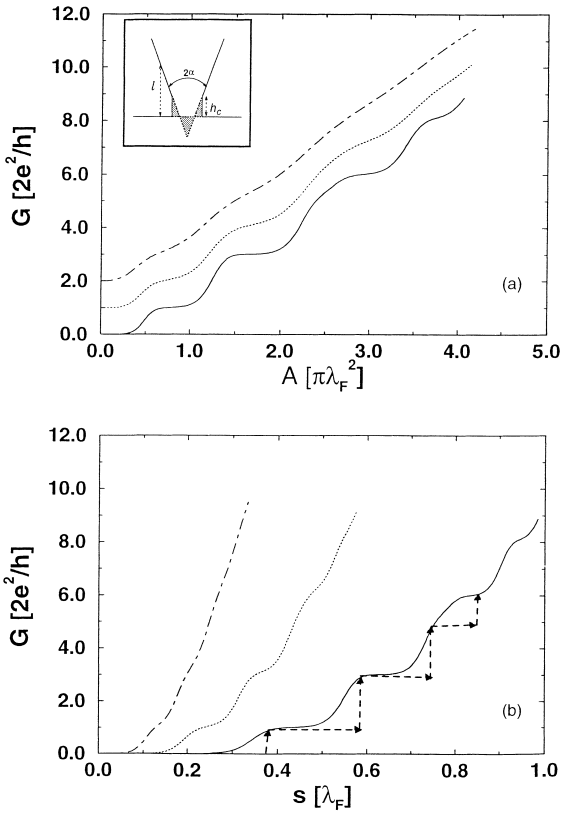

Fig. 2. The variation of the conductance G as a function of the contact cross-section A and tip displacement s are shown in (a) and (b), respectively. The tip and sample described by the continuum model is shown by the inset. Continuous, dotted and dash–dotted curves correspond to the cone angle $2\alpha = 60°$, 90°, 120°, respectively. For the abrupt interface growth, *G(s)* is schematically shown by the dashed line in (b).

of G with the push of the tip, *s (G(s))* one gets a perfect step structure. The only allowed values are [8, 9], $2e^2/h$, $6e^2/h$, $10e^2/h$, $12e^2/h$… corresponding to $n_i = 1,2,2,1,\ldots$ for $i = 1,2,3,4,\ldots$ in equation (3). Clearly, a realistic contact has finite length and hence the variation of G with the displacement of the tip, s or with the cross-section, A should differ from conditions considered either in the uniform constriction or in the quantum Sharvin case. If $l < \lambda_F$ the step structure is smeared out by the tunneling contribution. In a realistic potential, which includes saddle point effect, opening of channels is delayed and channel mixing becomes significant.

Let us now consider a realistic contact in more detail. To this end we simulated the contact between a Ni(111) tip on approaching the Cu(001) substrate by the state of the art molecular dynamics method using the embedded atom potential [30,31]. The atomic structure of the contact interface is illustrated in Fig. 1 for different values of s. The important results revealed from the atomistic simulation is that the contact of a sharp tip starts with a single atom, but grows discontinuously to include 4, 13 and 15 atoms. The shape of the contact area changes irregularly and the cross-section *A(s)* varies in a discontinuous fashion. Since the conductance is a function of the contact cross-section and each atom at the interface contributes to the total conductance by a significant fraction [6–11,32] of $2e^2/h$, one expects a close correlation between *G(s)* and *A(s)* curves.

Let us examine the behavior of *G(s)* for a realistic metal contact by using a simple model. We consider a conical tip with a cone angle 2α indenting to a metal surface within the incompressible jellium approximation. Since the volume is assumed to be conserved during the growth of the contact, we assume that the excess material (equivalent to the apex of the tip already dipped into the surface) is shifted to the contact interface to form a cylindrical neck of height h_c, and uniform cross-section A. Although *A(s)* varies with z and its shape deviates from circular symmetry, for simplicity we assume a uniform neck with circular symmetry. To express the electronic states quantized in the contact in an analytical form we further simplify the potential $V(\vec{r})$ in the following form:

$$V(\vec{r}) = \begin{cases} 0 & \rho \le R_c(z) \\ \infty & \rho > R_c(z) \end{cases} \qquad (5)$$

in the region $0 \le z \le l$ and $l > h_c$. Here $z \le 0$ is substrate and $\rho = (x^2 + y^2)^{1/2}$

Earlier SCF calculations [10] of the potential in a single Al atom contact revealed a parabolic variation for $V(\vec{r})$ in the transversal plane. However, the infinite wall potential is more appropriate for contacts including few atoms in the interface. We divide the above potential into N sections so that in each one $z_p < z < z_{p+1}$, $R_c(z) = R_c(z_p)$ and $A(z) = \pi R_c^2(z_p)$. We then express the electronic states quantized in each section by the circularly symmetric transversal wave, $\Phi_i(\rho, z_p)$ confined to the region $\rho \le R_c(z_p)$ and longitudinal wave, $\exp[i\gamma_i(z_p)z]$. The current

transporting state $\Psi(\vec{r},\vec{k})$ corresponding to a free electron that enters into the contact with energy $E = \hbar^2k^2/2m^*$ and finite momentum in the propagation direction $\hbar k_z$, is expressed in each section, $z_p < z \leq z_{p+1}$ in terms of the linear combination of states quantized in this particular section,

$$\Psi(\vec{r},\vec{k})|_{z_p\leq z<z_{p+1}} = \sum_i [A_i(z_p,\vec{k})\Phi_i(\rho,z_p)e^{i\gamma_i(z_p)z} + B_i(z_p,\vec{k})\Phi_i^*(\rho,z_p)e^{i\gamma_i(z_p)z}] \quad (6)$$

The coefficients $A(z_p,\vec{k})$ and $B(z_p,\vec{k})$ are determined by the multiple boundary matching [10] using the transfer matrix method. The current operator is evaluated and summed over the Fermi surface to find the current *I*. The conductance *G* is calculated as a function of *A* or *s* using the linear response theory.

Fig. 2(a) presents our calculated *G(A)* results for three different cone angles. As expected, for larger 2α values (h_c becomes smaller), *G(A)* tends to lose all structure. Similar behavior is seen for *G* vs *s* in Fig. 2(b). In obtaining these results, it is assumed that *A* increases continuously with *s*. In reality though, *A* changes discontinuously as has been demonstrated by atomistic simulation [31]. Hence *G* must vary discontinuously and should show a jump whenever *A(s)* increases suddenly by incorporation of new atoms into the interface (see Fig. 1). This variation is schematically illustrated in Fig. 2(b) by dashed lines. Owing to the single atom migration to or from the interface (or upon atomic rearrangements within the interface) between two consecutive jumps of *A(s)*, the conductance may change by significant fraction of $2e^2/h$. This causes the plateaus to disappear. The behavior predicted by the present analysis is in agreement with the *G(s)* curves measured experimentally [3,4,5]. Other experiments providing simultaneous force and conductance measurements in a metal constriction [20–22] and theoretical calculations based on realistic potentials [8,9,23,24] also support the present interpretation.

The disordered atomic structure at the interface delays the opening of channels due to the increased backscattering [10, 34, 35]. The metal contact having only one atom at the interface is a special case, since the conductance through this atom strongly depends on the electronic structure of the free atom and its bonding structure to the left and right side [32,33]. In the other extreme case where *A* is large and incorporates many atoms in the interface, the semiclassical picture as formulated by Sharvin is valid. Lastly, due to the irregular shape of the layers at the close proximity of the contact, the adiabatic approximation, where the energy of the state $\Phi_i(\rho,z_p)$ can be expressed as a smoothly varying function $\epsilon_i(z_p)$ is not valid.

In summary, *G(s)* not only depends on the cross-section of the contact but also on its detailed atomic structure. The quantization of electronic motion in the constriction is reflected in the variation of *G(s)*, but the sudden jumps are attributed to the sudden changes of *A(s)*.

4. Contacts on graphite surface

Graphite is a semimetal which exhibits strongly directional electronic and mechanical properties. Each C (Carbon) atom with its three planar sp^2-hybrid orbitals (formed from the combination of *s*, p_x and p_y, atomic orbitals) is bonded to the three nearest neighbor C atoms. This way, the C atoms are arranged in the honeycomb structure in the (*xy*)-plane and they make the individual graphite plane (or graphene).

The graphite solid forms by the stacking of the graphene along the *z*-direction with wide interplanar separation, $d \sim 3.35$ Å. In the normal stacking sequence (of Bernal graphite), adjacent planes are shifted relative to each other so that three alternating (α-)atoms of a hexagon face directly three atoms in the adjacent graphenes. The remaining three (β-) atoms face the centers of the hexagons of the graphenes lying above and below this plane. The strong bonding combination of two neighboring sp^2-hybrid orbitals leads to the nearest neighbor distance (i.e. the C–C distance of a hexagon) which is rather short (1.4 Å). The cohesion is strong (7 eV/atom) within the graphene. On the other hand, the interplanar interaction is weak and mainly occurs through the small overlap $\langle p_z|H|p_z'\rangle$ between the α-atoms in the adjacent layers, and partly by the Van der Waals interaction.

The above directional behavior is reflected in the electronic properties and the electronic energy band structure. The σ-bands due to the sp^2-hybrid orbitals lie in the range of 2–20 eV below E_F. The π-bands

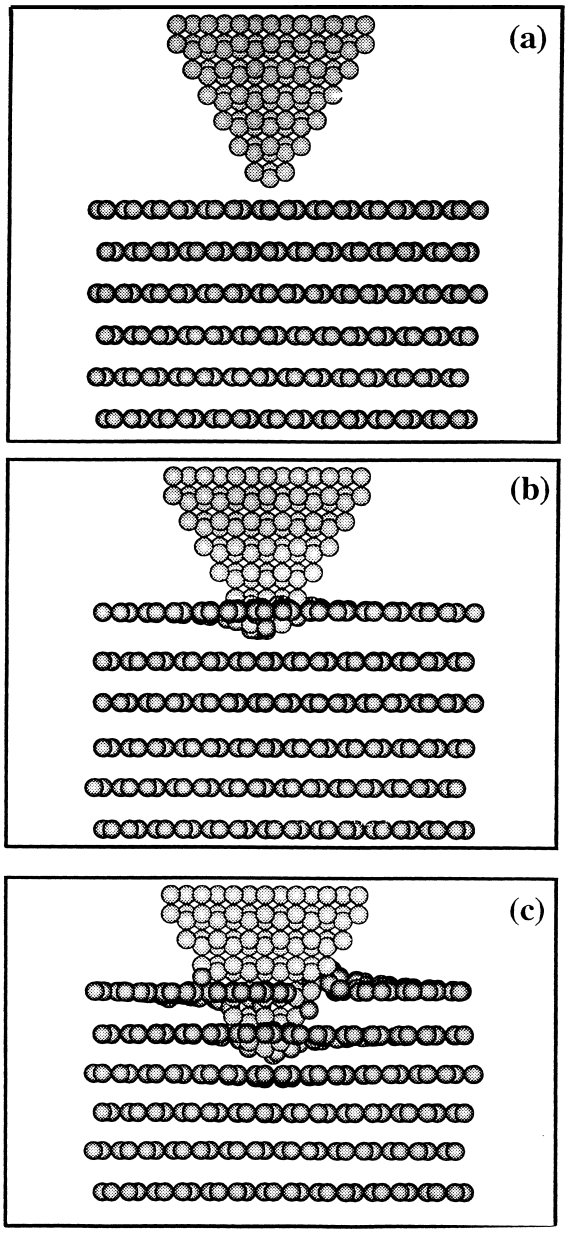

Fig. 3. The side views of the atomic structure of contact created by a hard tip on the graphite planes. Atomic positions are calculated by using the molecular dynamics method performed at $T = 4$ K. (a) Before the contact is set in; (b) the first layer is punctured; and (c) the contact is made in the second layer.

due to the p_z, orbitals lie close to E_F. Since the interlayer interaction is rather weak, the σ- and π-bands of a single graphene are only slightly modified when full graphite structure is included. Along the k_z-direction, for example, the four π-bands near the Fermi level show the effect of the interplanar interaction. Two of these bands π_α and π_α*, originate from the bonding and antibonding of p_z-orbitals between atoms in adjacent planes; each has a dispersion of 1 eV. The other two, π_β and π_β* are dispersionless and degenerate due to the negligible interaction between p_z-orbitals of β-atoms. These overall features, revealed by many earlier studies [36–38], show that graphite is a semimetal with low total density of states, D(E) at the Fermi level.

The weak interplanar bonding, low $D(E_F)$ and two types of C atoms (α- and β-types) have also been deduced from the STM experiments performed in tunneling regime. In the normal tunneling operation of STM three atoms of the hexagon were imaged. The level of tunneling current I was low even at small tip–sample distance. In the topographic mode operating at small tip–sample distance, the line scans exhibited "giant" corrugations [39]. These interesting results have been a subject of further investigations and have been explained by theoretical studies [39,40].

The variation of conductance through an atomic size contact created by an STM on the graphite surface has exhibited unusual behavior. In contrast to that of the contact on other metals, G did not increase as the tip pushed towards the graphite surface. Instead G jumped between two different values in some quasiperiodic fashion. This behavior is different from that of Sb which also has low $D(E_F)$ as in graphite. It is clear that the continuum model used for the normal metal contacts cannot be applied to graphite.

The unusual behavior of *G(s)* can be deduced from the detailed knowledge of atomic and electronic structure which are modified in the course of contact formation. To this end, we first investigate the evolution of contact created by a hard tip by using MD method. We use Tersoff potential [41] extended for multilayer graphite [42]. The results for three different values of s are shown in Fig. 3. Three features are important in these atomistic simulations. As the hard tip approached the surface, the top atomic plane is first attracted upwards. Later it is pressed downwards and

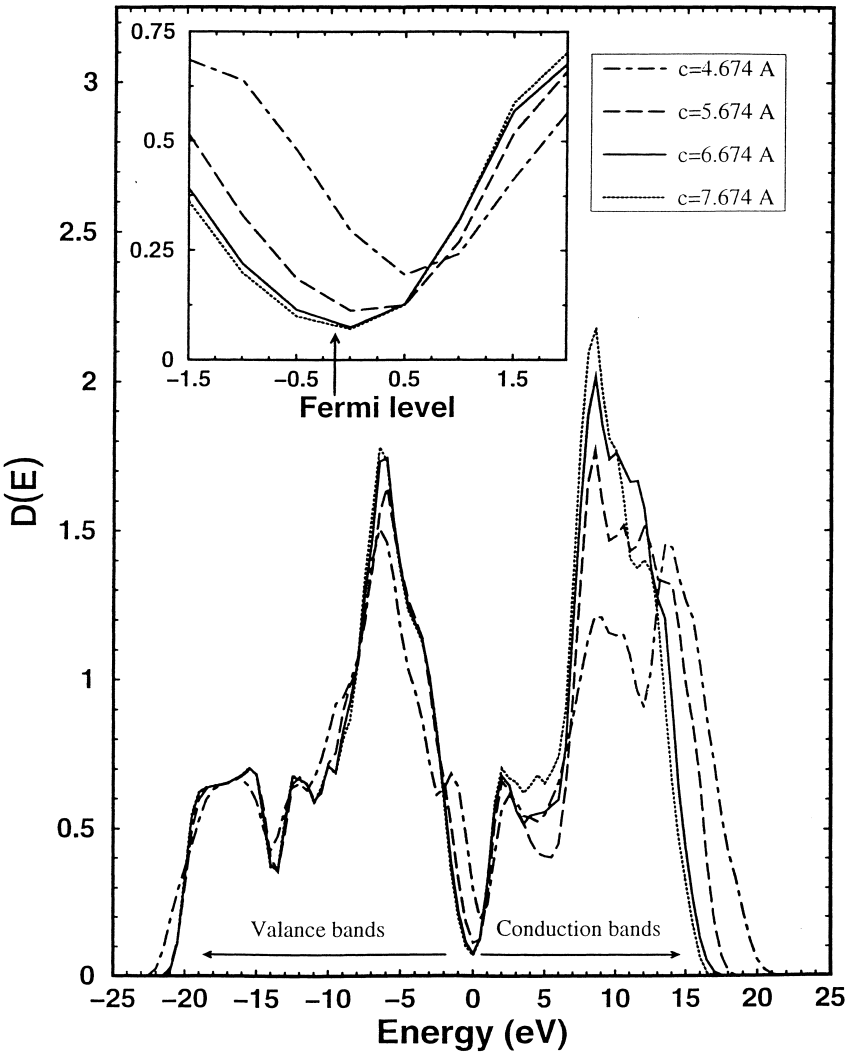

Fig. 4. Densities of states D(E) (States/eV per unit cell) is calculated as a function of the lattice parameter c (that is twice the interlayer distance d). The variation of $D(E_F)$ is highlighted by the inset.

the interplanar distance is reduced locally. Eventually the top layer is punctured, releasing the strain, and the apex of the tip dips into the interlayer region. Depending on the shape of the tip and its position on the graphene, the puncture occurs either as a local plastic deformation or as local breaking of graphene into flakes. As the tip is pushed further, the above sequence of events repeats.

The effect of the above local deformation induced by a hard tip pressing towards graphite surface was further explored by the SCF pseudopotential [43] calculations in momentum space within local density approximation [44]. By using the kinetic energy cutoff, $|\vec{k}+\vec{G}|^2 \leq 37Ry$ we calculated total energy E_T, energy band structure $E_n(\vec{k})$ and the density of states D(E) of graphite by varying the interlayer distance d. The band structure at equilibrium d and the variation of E_T with d are in good agreement with earlier calculations [38]. Reducing d under uniaxial strain caused the dispersion of bands along the k_z-direction to increase and the Fermi surface to enlarge. Moreover, because of increased interlayer interaction

between p_z-orbitals, the occupied π_β-band in the ($k_x k_y$)plane moved upwards and and crossed E_F. The effect of these modifications on D(E) is illustrated in Fig. 4. As d (which is equal to one half of the lattice parameter c) decreases, $D(E_F)$ increases. In fact $D(E_F)$ increases by a factor of three upon decreasing d by $\sim$ 1 Å. This is an important feature that influences the electron transport and plays a crucial role in determining *G(s)*. A rigorous calculation of *G(s)* curve for a graphite contact is very tedious. It requires the knowledge of the self-consistent potential as well as the electronic wave functions quantized at the close proximity of the contact. Neither the model calculations used for normal metals, such as nearly free electron, nor tightbinding calculations are appropriate.

By combining the results of atomistic simulations of contact and the density of states calculations, we propose a mechanism for understanding the peculiar behavior of the conductance through a contact on graphite surface. Owing to the low $D(E_F)$, the opening of the first ballistic channel may not occur for a sharp tip [45,46]. At the initial stage of the contact, $D(E_F)$ is even lower than that of the bulk graphite since the surface atoms are attracted by the tip and hence d has slightly increased. As the tip continues to press towards the graphite surface, d, decreases locally. Hence $D(E_F)$ of the region where the electrons are transferred increases. Since the current is

$$I \propto \int_{E_F}^{E_F + e\Delta V} dE D(E) T(E) \qquad (7)$$

where T is the transmission coefficient, the conductance gradually increases with decreasing s until the apex makes a hole on the surface. Once the atomic plane is punctured by the comprehensive strain is relieved and $D(E_F)$ falls back towards its normal low value. Hence I and G under constant bias voltage decrease abruptly when the tip punctures through the top plane. Here we assume that the current from the tip to the punctured layer is negligible. Having punctured through, the tip faces a new graphene and the same sequence of events (which occurred for the first graphene) repeats itself and thus G varies quasi periodically with s. Owing to the interaction between the tip and punctured graphene atoms, or deformation of the apex, some irregularities may be superimposed on the periodic variation of *G(s)*. The average value of the conductance can also increase due to the increased diffused conductance from the lateral layers. The model calculation of conductance has been performed recently [47].

5. Conclusion

We have investigated the conductance through a contact created by an STM tip pushed on metal surfaces. We considered two cases: a normal metal and graphite. The atomistic simulations, based on the molecular dynamics method, indicate that the shape of the contact on the graphite surface is very different from that of a tip on Cu. The contact interface on the metal surfaces grows discontinuously leading to sudden jumps in conductance of around $2e^2/h$. But when a tip approaches graphite, the interlayer distance first increases, then decreases and eventually the tip punctures the surface. This sequence of events essentially repeats as the tip faces new graphene. Using the results of electronic structure calculations of graphite under strain, we proposed a mechanism of electron transport through the contact on graphite that successfully explains the experimental results.

References

[1] I.P. Batra, C.R. Brundle, Surface Science 57 (1976) 12.
[2] M. Chen, I.P. Batra, C.R. Brundle, J. Vac. Sci. Technol 16 (1979) 1216.
[3] J.K. Gimzewski, R. Möller, Phys. Rev. B36 (1987) 1284.
[4] J.K. Gimzewski, R. Möller, D.W. Pohl, R.R. Schlitter, Surface Science 189 (1987) 15.
[5] U. Dürig, J.K. Gimzewski, D.W. Pohl, Phys. Rev. Lett. 57 (1986) 2403.
[6] N.D. Lang, Phys. Rev. B36 (1987) 8173.
[7] J. Ferrer, A. Martîn Rodero, F. Flores, Phys. Rev. B38 (1988) 10113.
[8] S. Ciraci, E. Tekman, Phys. Rev. B40 (1989) 11969.
[9] S. Ciraci, in Scanning Tunneling Microscopy and Related Methods, edited by R.J. Bohm, N. Garcia and H. Rohrer, p113, Kluwer Academic Publishers, Volume 184 (1990).
[10] E. Tekman, S. Ciraci, Phys. Rev. B43 (1991) 7145.
[11] T. N. Todorov, A.P. Sutton, Phys. Rev. Lett. 70 (1993) 2138 .
[12] A.P. Sutton, J.B. Pethica, J. Phys. Condensed Matter 2 (1990) 5317.
[13] U. Landman, W.D. Luedke, N.A. Burnham, R.J. Colton, Science 248 (1990) 454.
[14] U. Landman, W.D. Luedke, J. Vac. Sci. Tech. 9 (1991) 414.
[15] N. Agraït, J.G. Rodrigo, S. Vieria, Phys. Rev. B47 (1993) 12345.

[16] J.I. Pascual, J. Mendez, J. Gomez-Herrero, A.M. Baro, V.T. Binch, N. Garcia, Phys. Rev. Lett. 71 (1993) 1852.
[17] J.I. Pascual, J.I. Mendez, J. Gomez-Herrero, A.M. Baro, N. Garcia, U. Landman, W.D. Luedke, E.N. Bogachek, H.P. Cheng, Science 267 (1995) 1793.
[18] J.M. Krans, C.J. Muller, N. van der Post, F.R. Postama, A.P. Sutton, T.N. Todorov, J.M. Ruitenbek, Phys. Rev. Lett. 74 (1995) 2146.
[19] A.M. Bratkovsky, A.P. Sutton, T.N. Todorov, Phys. Rev. B52 (1995) 5036.
[20] N. Agraït, G. Rubio, S. Vieira, Phys. Rev. Lett. 74 (1995) 3995.
[21] G. Rubio, N. Agrait, S. Vieira, ibid, 76 2302 (1996).
[22] A. Stalder, U. Durig, App. Phys. Lett. 68 (1996) 637.
[23] H. Mehrez, S. Ciraci, C. Y. Fong and S. Erkoc, J. Phys.: Condensed matter 9 (1997) 10843.
[24] H. Mehrez and S. Ciraci, J. Phys. B56 (1997) 12632.
[25] J. K. Gimzewski and A. Oral (private communications).
[26] I.P. Batra, Surface Science, 395 (1998) 43.
[27] B. J. van Wees, H. van Houten, C.W.J. Beenackker, J.G. Williams, L.P. Kouwenhowen, D. van der Marel, C.T. Foxon, Phys. Rev. 60 (1988) 848.
[28] D.A. Wharam, T.J. Thornton, R. Newbury, M. Pepper, H. Ritchie, G.A.C. Jones, J. Phys. C21 (1988) L209.
[29] Yu. V. Sharvin, Zh. Eksp. Teor. Fiz. 48, 984 (1965) [Sov. Phys.JETP21, 655 (1965) 1.
[30] M.S. Daw, M.I. Baskes, Phys. Rev. B29 (1984) 6443.
[31] A. Buldum, S. Ciraci, I. P. Batra, Phys. Rev. B57 (1998) 2468.
[32] H Mehrez, S. Ciraci, A. Buldum, I.P. Batra, Phys. Rev. B 55 (1997) R1981.
[33] N.D. Lang, Phys. Rev. Lett. 79 (1997) 1357.
[34] E. Tekman, S. Ciraci, Phys. Rev. B40 (1989) 8559.
[35] I. Kander, Y. Imry, U. Sivan, Phys. Rev. B41 (1990) 12941.
[36] R.C. Tatar, S. Rabii, Phys. Rev. 25 (1982) 4126.
[37] J.C. Charlier, X. Gonze, J.P. Michenaud, Phys. Rev. B43 (1991) 4579.
[38] M.C. Schabel, J.L. Martins, Phys. Rev. B46 (1992) 7185.
[39] J. M. Soler, A.M. Baro, N. Garcia, H. Rohrer, Phys. Rev. Lett. 57 (1986) 444.
[40] I.P. Batra, N. Garcia, H. Rohrer, H. Salamink, E. Stall, S. Ciraci, Surf. Sci. 181 (1987) 126.
[41] J. Tersoff, Phys. Rev. Lett. 61 (1988) 2879.
[42] K. Nordlund, J. Keinonen, T. Mattila, Phys. Rev. Lett. 77 (1996) 699.
[43] G.B. Bachelet, D.R. Hamann, M Schlüter, Phys. Rev. B26 (1982) 4199.
[44] D. M. Ceperley, B.J. Alde, Phys. Rev. Lett. 45 (1980) 566.
[45] I.P. Batra, S. Ciraci, Phys. Rev. B36 (1987) 6194.
[46] D. J. Marti, Ph. D. Thesis, ETH Zurich (1986).
[46] Ç. Kiliç, H. Mehrez, S. Ciraci, Phys. Rev. B58 (1998) 7872.
[47] Ç. Kiliç, H. Mehrez, S. Ciraci, Phys. Rev. B58 (1998) 7872.